Journal of Alloys and Compounds 505 (2010) 733–738

Contents lists available at ScienceDirect

Journal of Alloys and Compounds

journal homepage: www.elsevier.com/locate/jallcom

Investigation of diphasic region in the $Pr_2O_3 + Sm_2O_3$ mixed oxide system at various temperatures

D. Vijayalakshmi[a,b], N.V. Chandra Shekar[b,*], S. Ramya[c], P.Ch. Sahu[b], G. Meenakshi[a]

[a] Department of Physics, Kanchi Mamunivar Centre for PG & Research Studies, Govt. of Pondicherry, Lawspet 605008, Pondicherry, India
[b] High Pressure Physics Section, Condensed Matter Physics Division, Indira Gandhi Centre for Atomic Research, Kalpakkam 603102, Tamil Nadu, India
[c] Corrosion Science and Technology Division, Metallurgy and Materials Group, Indira Gandhi Centre for Atomic Research, Kalpakkam 603102, Tamil Nadu, India

ARTICLE INFO

Article history:
Received 19 October 2009
Received in revised form 18 June 2010
Accepted 23 June 2010
Available online 1 July 2010

PACS:
81.05.Je
64.75.Nx
81.30.Dz
61.05.Cp
78.30.−j

Keywords:
Mixed rare-earth oxides
Phase transitions
X-ray diffraction
Micro-Raman spectroscopy

ABSTRACT

X-ray diffraction studies on mixed rare-earth oxides Pr_2O_3 and Sm_2O_3 quenched at various temperatures were carried out and their phase relationship was analyzed. Mixtures of Pr_2O_3 and Sm_2O_3 at different compositions were heated at various temperatures in the range 500–1200 °C and then air quenched. The structures of these quenched samples were analyzed using X-ray diffraction and Raman spectroscopy. Pure Pr_2O_3 and Sm_2O_3 exhibit C-type cubic phase at NTP. While Pr_2O_3 retains its cubic phase up to 1200 °C, the Sm_2O_3 transformed to B-type monoclinic phase above 800 °C. However, their mixtures when heated at different temperatures showed interesting structural behaviour. For the mixture up to 40 wt.% of Sm_2O_3 in Pr_2O_3, no significant change was observed at lower temperatures (~800 °C), and the C-type cubic phase was observed. As the ratio was gradually increased above 40%, a diphasic region in the range 50–70% was observed, with a combination of both C-type cubic and B-type monoclinic phases. When the temperature was raised to 1200 °C, the 80% of Sm_2O_3 shows a complete structural transition from cubic to monoclinic phase. Based on the analysis of our results various crystal structures and stability regimes of mixed oxide have been reported.

1. Introduction

The rare-earth oxides (Ln_2O_3) are widely used in the field of metallurgy, nuclear technology, optoelectronics for lasers, etc. [1–3]. Studies about the polymorphism of rare-earth oxides have become an important area of research. It is important for understanding the thermodynamic phase changes and intermediate phase of these compounds as a function of temperature. Rare-earth oxides show five polymorphic modifications, namely, A-, B-, C-, H- and X-type. At ambient conditions, the A-type hexagonal (space group: *P*-3*m*1, no. 164) is the stable structure for the oxides of lighter rare earths from La–Pm, while the oxides of medium rare earths may exist either in the B-type monoclinic or C-type cubic structure. It has been found that these medium rare-earth oxides have the monoclinic distortion of the C-type structure. The thermodynamic stability of these C-type medium rare-earth oxides like Sm_2O_3, Eu_2O_3 and Gd_2O_3 at lower temperatures is under debate. The C-type cubic is the characteristic structure (also called as bixbyite structure) for heavier rare-earth oxides from Tb–Lu (space group: *Ia*-3, no. 206). The H-type hexagonal and the X-type cubic Ln_2O_3 exist only at very high temperatures. Above 2000 °C, the H- and X-type phases are stable, whereas the A-, B- and C-type phases are commonly observed below this temperature [4,5].

These rare-earth oxides are broadly divided into two groups such as mixed and refined oxides. The mixed oxides are thermally stable and chemically active. These mixed oxides are widely used in making misch metal, glass abrasives, catalysts (fluid catalytic cracking, auto exhaust gas cleaning), iron and steel and cast iron additives, etc. [6]. These also have been used in the preparation of phosphors, solid state fuels and electro-chromic windows [7,8], in leather pigmentation and ash tracers for soil erosion aggregate studies [9,10]. Perovskite type rare-earth mixed oxides are well known for high temperature superconductors and ferro magnetic materials.

The proper understanding of polymorphic relationship among the various oxides is essential for any study involving these systems. A number of investigators have tried to explain the phase relationship among theses oxides at various temperatures and pressures, but several disagreements exist among all these studies [11–13]. Though much attention has not been paid to this problem,

* Corresponding author. Tel.: +91 44 27480347; fax: +91 44 2748008.
E-mail address: chandru@igcar.gov.in (N.V. Chandra Shekar).

0925-8388/$ – see front matter © 2010 Elsevier B.V. All rights reserved.
doi:10.1016/j.jallcom.2010.06.127

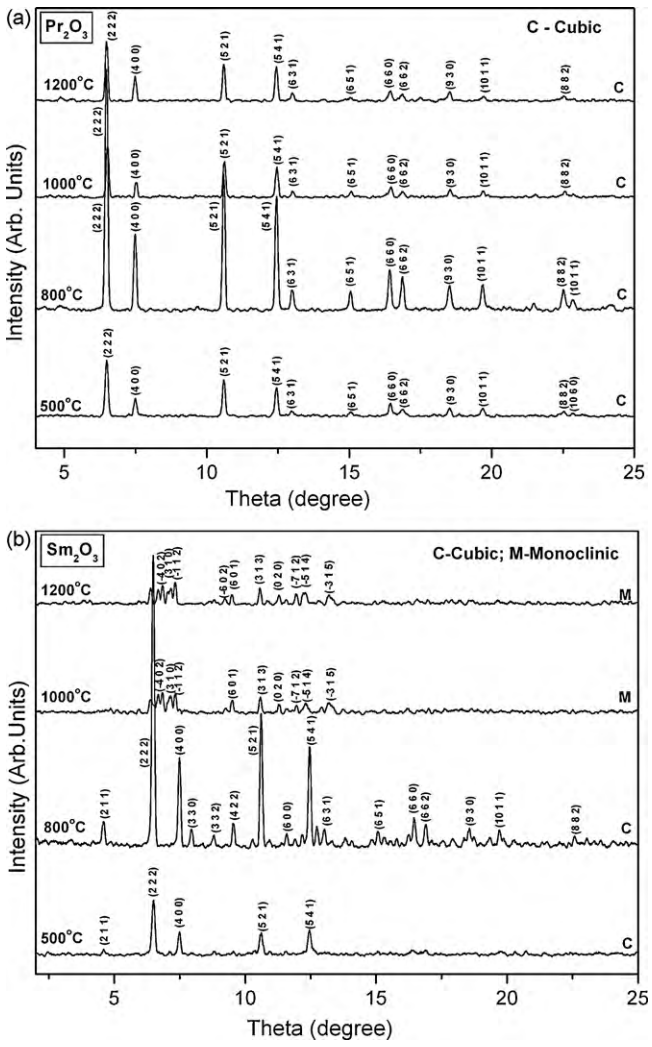

Fig. 1. (a) X-ray diffraction patterns of Pr_2O_3 at various temperatures. It is clearly indexed to the cubic phase. (b) X-ray diffraction patterns of Sm_2O_3 at various temperatures. This indicates a structural phase transition from cubic to monoclinic structure at 1000 °C.

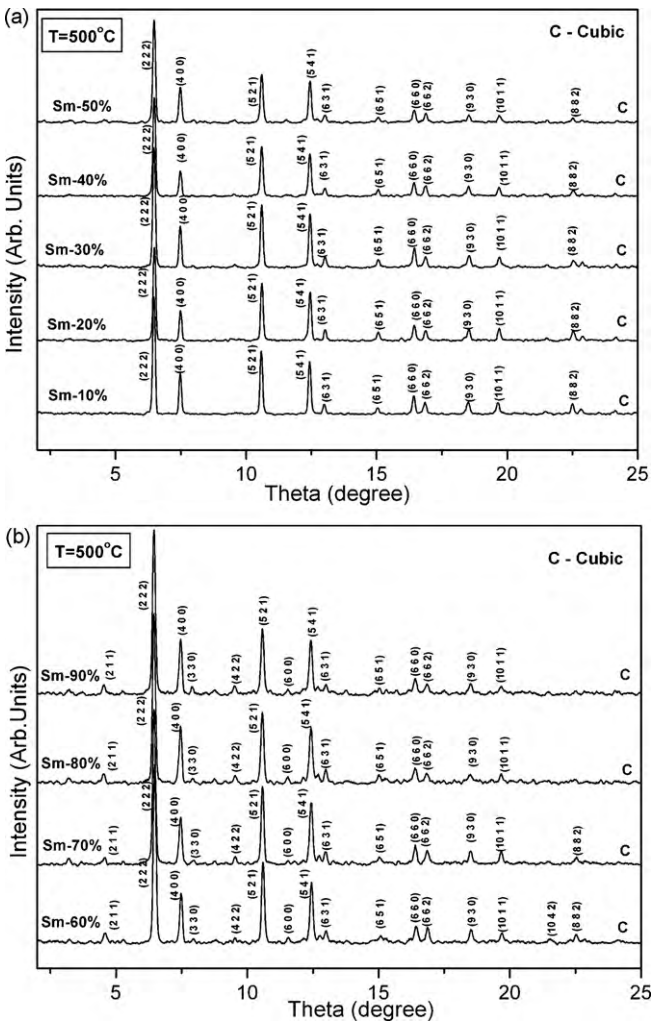

Fig. 2. (a) XRD patterns for various concentrations of Sm_2O_3 in Pr_2O_3 (10–50%) clearly show the cubic phase at 500 °C. (b) XRD patterns for various concentrations of Sm_2O_3 in Pr_2O_3 (60–90%) clearly shows the cubic phase at 500 °C.

the question still remains due to the inconclusive nature of the results reported. It is of special importance to study the reaction of rare-earth mixed oxides at elevated temperatures. Only a few combinations of these oxides have already been reported [14,15]. Several mixed oxides involving Pr_2O_3, Sm_2O_3, and Gd_2O_3, etc. have not been studied yet. The aim of our present work is to determine the phase details of the Pr_2O_3–Sm_2O_3 mixed oxide with respect to temperature by using X-ray diffraction (XRD) and micro-Raman spectroscopy as the experimental techniques.

2. Experimental

The rare-earth oxides used in the present study were obtained from Indian Rare Earth Ltd., India. The starting materials were of purity ~99.9%. The starting materials were characterized and it was found that Pr_2O_3 stabilized in cubic phase with space group *Ia*3 and lattice parameter $a = 10.93$ Å. The powder diffraction data of this sample has been accepted by International Centre for Diffraction Data (ICDD) with reference number W26425. All the samples indexed to cubic phase in our experiment were matched with this data. Samarium sesquioxide (Sm_2O_3) stabilized in the monoclinic phase with space group $C2/m$ and lattice parameters: $a = 14.1$ Å, $b = 3.6$ Å and $c = 8.8$ Å. This data matched well with PDF file no. 43-1030 of ICDD. Further all the samples indexed to monoclinic phase are matched to this powder data. The pure oxides as well as the mixtures were annealed in a silicon carbide box-type resistance furnace at various temperatures ranging from 500 to 1200 °C for 24 h, after which the samples were air quenched.

The X-ray diffraction patterns for all the samples were carried out by a Huber-Guinier diffractometer [16] which is in the vertical configuration with a Seeman-Bohlin focusing circle of diameter 114.6 mm. It is attached with a curved type quartz crystal monochromator and a scintillation detector for obtaining the XRD patterns. The incident X-ray beam is obtained from an 18 kW rotating anode X-ray generator (RAXRG) with a molybdenum target of wavelength $\lambda = 0.70926$ Å.

To study the effect of structural phase transformations on Raman modes, one batch of samples quenched from 1000 °C were investigated by micro-Raman spectroscopy using a HR 800 Horiba Jobin Yvon Raman imaging microscope. The system consisting of an Olympus optical microscope with 10× long distance objective was used to focus the beam on the sample. An Ar-ion laser operating at a wavelength of 488 nm was used as the excitation source and the laser spot size was approximately 3 μm in diameter and power was 8 mW at the sample. The slit width of the monochromator was 300 μm which corresponds to a resolution of 4 cm^{-1} and the spectra were collected in the wave number range 100–2000 cm^{-1}.

3. Results and discussions

On visual inspection, the pure Pr_2O_3 was black and Sm_2O_3 appeared to be white in colour. When Sm_2O_3 was added to Pr_2O_3, its colour slowly changed and the white colour began to appear at the higher percentage of Sm_2O_3. Up to 40% of Sm_2O_3 in Pr_2O_3, the black colour was dominating. Slowly the colour changed from black to brown when Sm_2O_3 was increased to 50%. The brown colour remained up to 70% of Sm_2O_3 added to Pr_2O_3 and then changed to dirty white at 80–90% of Sm_2O_3.

The phase identification of mixed rare-earth oxides in the present study was carried out by using XRD. Figs. 1–5 show the

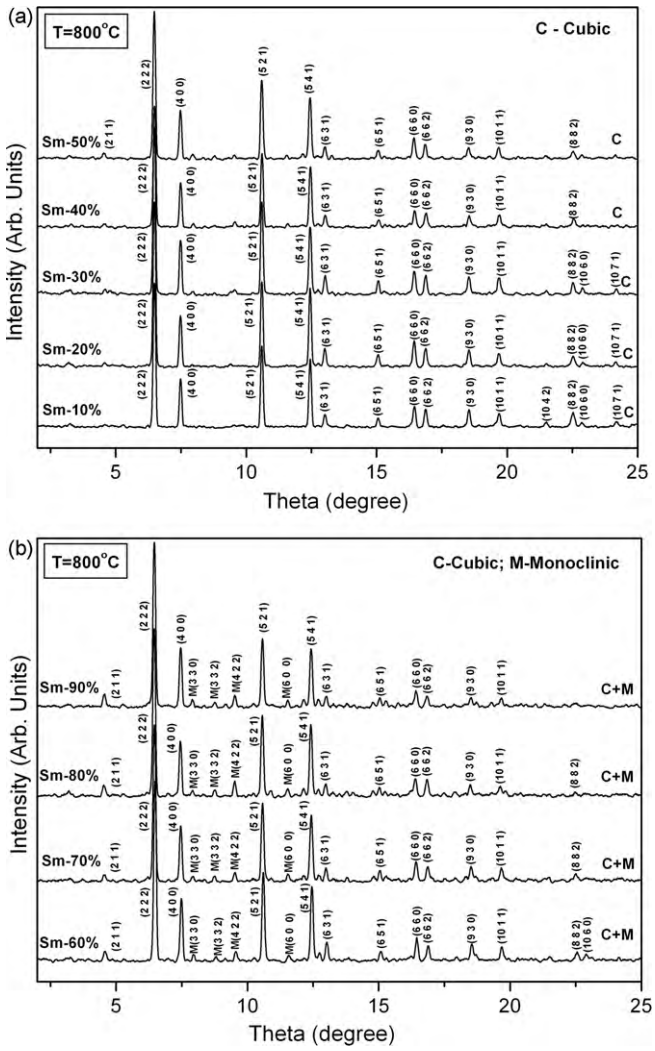

Fig. 3. (a) XRD patterns for different concentrations of Sm_2O_3 in Pr_2O_3 (10–50%) clearly shows the cubic phase at 800 °C. (b) XRD pattern of different concentrations of Sm_2O_3 in Pr_2O_3 (60–90%) showing the cubic phase with a slight monoclinic distortion of Sm_2O_3 at 800 °C. Here the monoclinic peak indices are distinguished as M(3 3 2), M(4 2 2), etc.

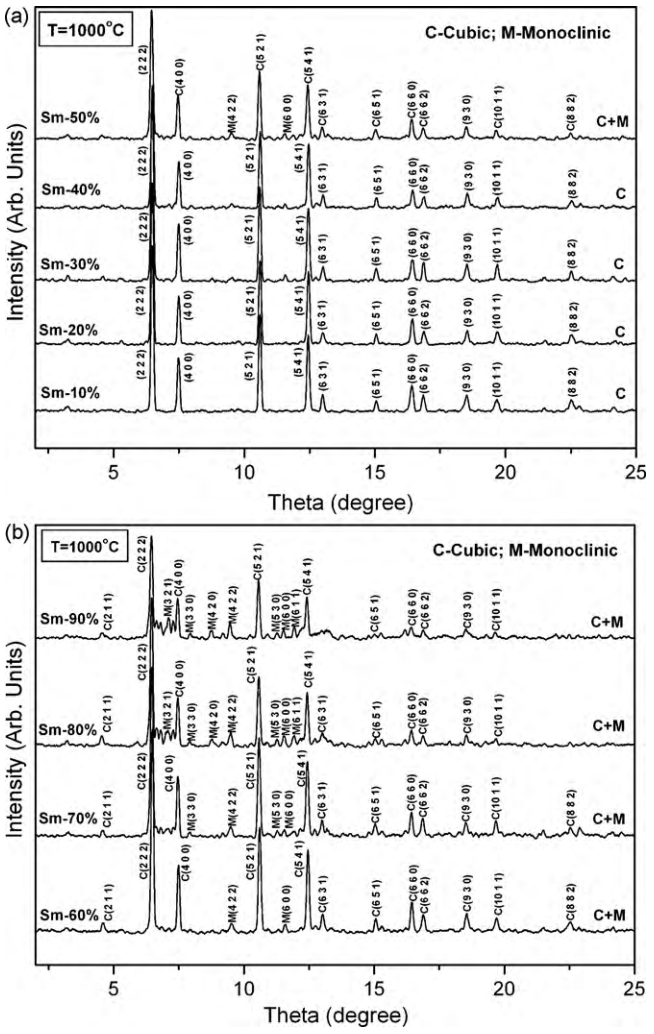

Fig. 4. (a) XRD pattern for various concentrations of Sm_2O_3 in Pr_2O_3 (10–50%) at 1000 °C showing the emergence of new diffraction peaks at 50% of Sm_2O_3. The cubic and monoclinic indices are distinguished as C(2 2 2), M(4 2 2), etc. (b) XRD pattern for various concentrations of Sm_2O_3 in Pr_2O_3 (60–90%) at 1000 °C showing the co-existence of two phases. The *h k l* indices corresponding to cubic and monoclinic phases are indicated as C(2 2 2), M(4 2 2), etc.

XRD patterns obtained for various compositions of the samples studied. Fig. 1(a) and (b) shows the XRD patterns of pure Pr_2O_3 and Sm_2O_3 samples at various temperatures ranging from 500 to 1200 °C. Fig. 1(a) shows that the C-type cubic phase for Pr_2O_3 is stable up to 1200 °C. This result is contrary to the earlier work [17], which reports a transition from cubic to hexagonal phase at higher temperatures. Fig. 1(b) shows the XRD patterns for Sm_2O_3 indicating the C-type cubic phase stable up to 800 °C, above which it transforms to the monoclinic phase. This result is in agreement with the earlier published reports [18–21].

Fig. 2(a) shows the XRD patterns for various compositions, starting from 10 to 50 wt.% Sm_2O_3 in Pr_2O_3 at 500 °C. The pattern clearly shows the C-type cubic phase up to 50% of Sm_2O_3. Fig. 2(b) shows the pattern for the remaining compositions (60–90% Sm_2O_3 in Pr_2O_3) at the same temperature. No structural phase change was observed at this temperature. Fig. 3(a) and (b) also reveals the same cubic structure at 800 °C for all the compositions (10–90%) with a slight monoclinic distortion of Sm_2O_3. The distortion was not observed at lower compositions and appeared only after the emergence of new diffraction peaks at 50% Sm_2O_3. It has been seen that in the case of Sm_2O_3, it undergoes a phase transition from cubic to monoclinic at higher temperatures (800–1000 °C). Obviously some monoclinic peaks may arise due to the above transition, but in our case the cubic phase was clearly indexed as shown in Fig. 3(b).

Fig. 4(a) shows the XRD patterns for various compositions of mixed oxides at 1000 °C. The pattern was found to be cubic up to 40% of Sm_2O_3 and above that, some new diffraction peaks characteristic of the monoclinic phase of Sm_2O_3 emerged. Starting from 50%, these peaks continue to remain through higher compositions at this temperature. A mixed phase of both cubic and monoclinic up to 90% of Sm_2O_3 has been shown in Fig. 4(b) clearly for 1000 °C.

Fig. 5(a) and (b) shows the XRD patterns at 1200 °C. In this plot, the observed pattern shows a C-type cubic phase up to 40% because of the dominant Pr_2O_3. At 50%, a two phase region was observed accompanied with the appearance of new diffraction peaks. At 80% of Sm_2O_3, a pure monoclinic was observed and this phase continued to remain at the higher composition of 90% Sm_2O_3.

In addition, the interplanar spacings '*d*' vs compositions graph also was plotted in Fig. 6. As the composition increases from 0 to 100% of Sm_2O_3, the *d*-values begin to decrease. This is clearly shown in the graph at a temperature of 1200 °C.

Micro-Raman studies on the mixed rare-earth oxides have also been carried out to confirm the results obtained by XRD studies.

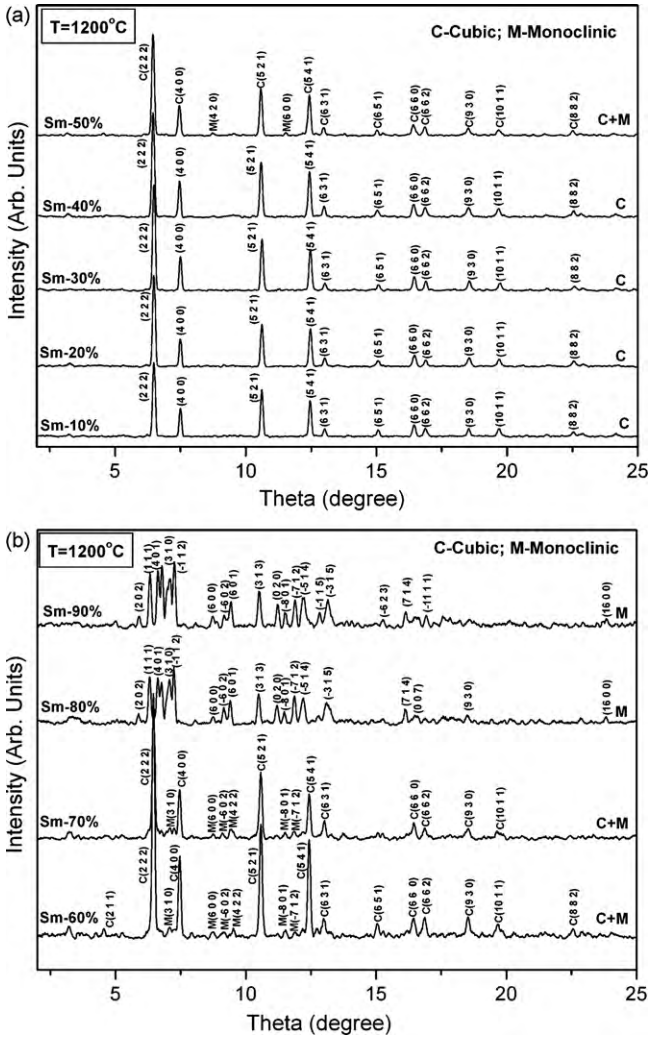

Fig. 5. (a) XRD pattern for various concentrations of Sm_2O_3 in Pr_2O_3 (10–50%) at 1200 °C. The pattern shows the emergence of monoclinic phase at 50% of Sm_2O_3. The mixed phase indices are distinguished as C(2 2 2), M(4 2 2), etc. (b) XRD patterns for different concentrations of Sm_2O_3 in Pr_2O_3 (60–90%) at 1200 °C, indicating a structural phase transition from cubic to monoclinic phase at 80% of Sm_2O_3. The cubic and monoclinic indices are indicated as C(4 4 4), M(4 2 2), etc.

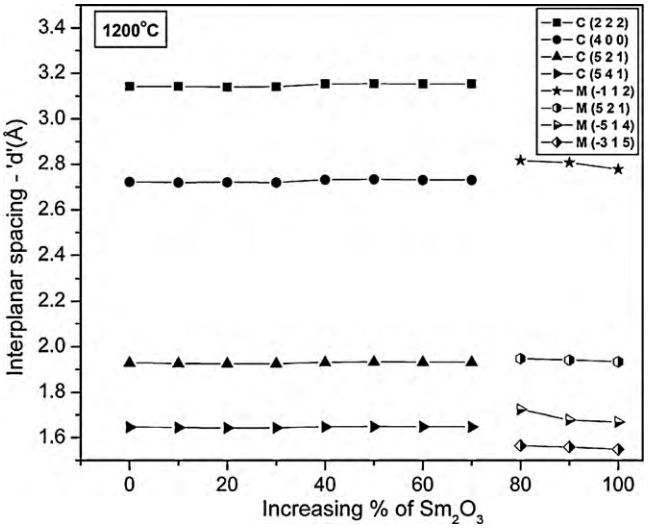

Fig. 6. The variation of *d* spacings with composition.

The results agree very well with that obtained in XRD studies. Fig. 7(a)–(c) shows the micro-Raman spectra of various compositions quenched from 1000 °C. The maximum intensities of the spectra were normalized. All the spectra were characterized by the presence of a very strong (cubic) band in the range 800–930 cm^{-1}. In addition to this high intensity band, there is a band at about 1050 cm^{-1}. Another band grows at about 590 cm^{-1} for 20% of Sm_2O_3. These modes grow prominent up to about 60% of Sm_2O_3 and thereafter, the peak at 1050 starts reducing and merges with a broader peak at 925 cm^{-1}. However, the peak at 590 cm^{-1} is retained even at highest concentration of Sm_2O_3. It is evident that the lattice mode at 590 cm^{-1} is influenced by the substitution of Sm atom in the lattice. The high intensity of the central band compared to others, indicates a large polarizability during the vibration. So this band is expected to be one of the most sensitive to the changes in the chemical bonding. For the first three compositions, the strongest peaks were observed at 839, 846 and 837 cm^{-1} respectively. As reported in the XRD, at higher concentrations of Sm_2O_3, a few peaks corresponding to the monoclinic phase are observed. In particular, the peak observed at 927 cm^{-1} is due to the C-type cubic phase while the peaks at 403 and 251 cm^{-1} are expected to be due to the monoclinic phase.

We have primarily monitored the changes in the most predominant cubic phase observed at 839 cm^{-1} and it clearly displayed a continuous shift to higher wave numbers up to 927 cm^{-1} with increase in Sm_2O_3%. At lower concentration of Sm_2O_3, intensities of the peaks of Pr_2O_3 were dominant. The weaker peaks of Pr_2O_3 broadened and disappeared with a gradual loss of intensity, as the weight percentage of Sm_2O_3 increased. The Sm_2O_3 peaks began to appear at nearly equal ratios of both the oxides, and then it started increasing as the concentration of Sm_2O_3 increased up to 90%.

The trend of increasing wave number of the most intense band across the period (Pr–Sm) can be explained in terms of lanthanide

Table 1
Summary of the structural information obtained from X-ray diffraction study of the mixtures of Pr_2O_3 and Sm_2O_3 heated at various temperatures.

S. no.	Sample	Phase composition at temperature			
		500 °C	800 °C	1000 °C	1200 °C
1.	Pr_2O_3	Cubic	Cubic	Cubic	Cubic
2.	90% Pr_2O_3 + 10% Sm_2O_3	Cubic	Cubic	Cubic	Cubic
3.	80% Pr_2O_3 + 20% Sm_2O_3	Cubic	Cubic	Cubic	Cubic
4.	70% Pr_2O_3 + 30% Sm_2O_3	Cubic	Cubic	Cubic	Cubic
5.	60% Pr_2O_3 + 40% Sm_2O_3	Cubic	Cubic	Cubic	Cubic
6.	50% Pr_2O_3 + 50% Sm_2O_3	Cubic	Cubic	Cubic + monoclinic	Cubic + monoclinic
7.	40% Pr_2O_3 + 60% Sm_2O_3	Cubic	Cubic	Cubic + monoclinic	Cubic + monoclinic
8.	30% Pr_2O_3 + 70% Sm_2O_3	Cubic	Cubic	Cubic + monoclinic	Cubic + monoclinic
9.	20% Pr_2O_3 + 80% Sm_2O_3	Cubic	Cubic	Cubic + monoclinic	Monoclinic
10.	10% Pr_2O_3 + 90% Sm_2O_3	Cubic	Cubic	Cubic + monoclinic	Monoclinic
11.	Sm_2O_3	Cubic	Cubic	Monoclinic	Monoclinic

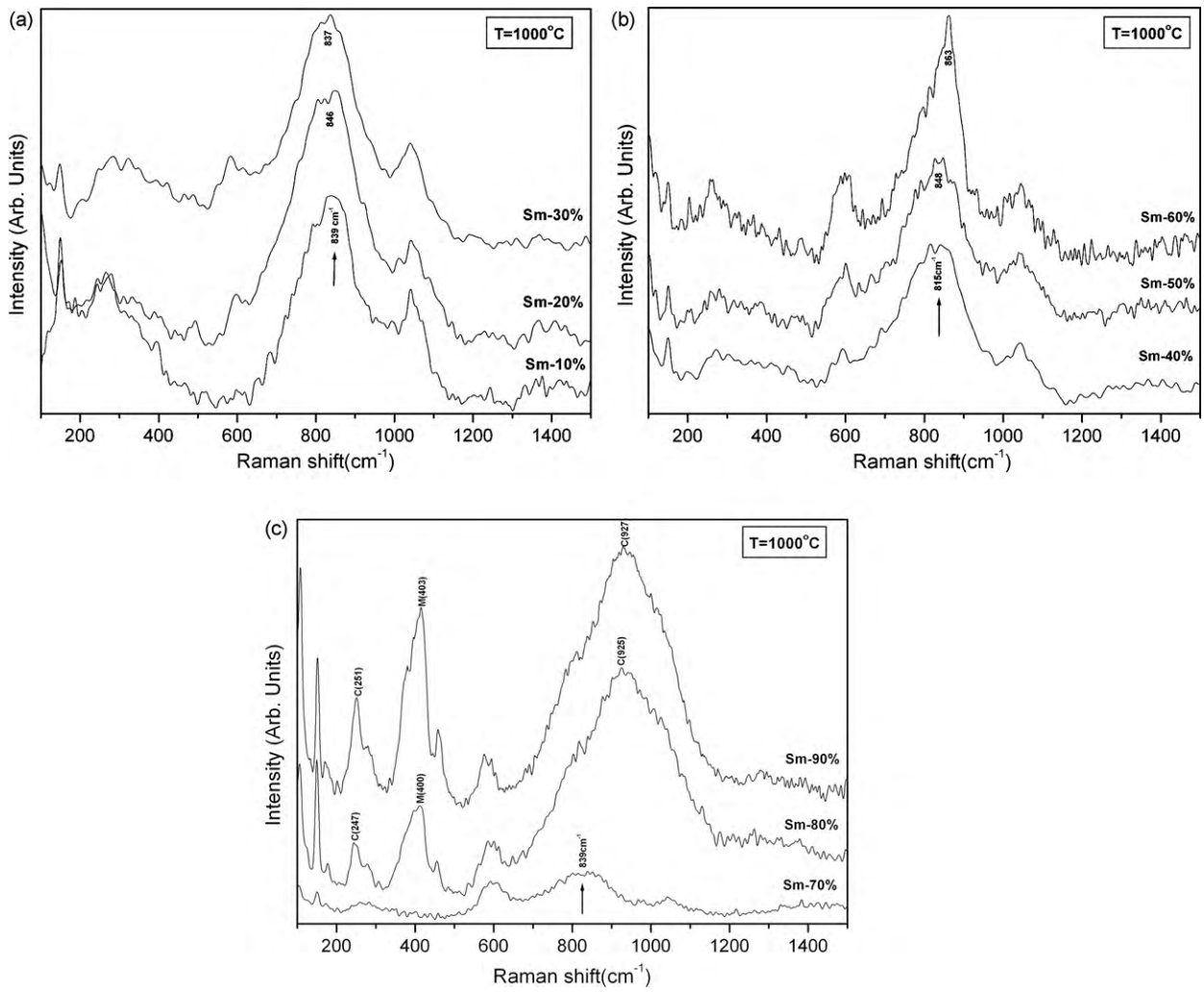

Fig. 7. (a) Micro-Raman spectra for different concentrations of Sm_2O_3 in Pr_2O_3 (10–30%) at 1000 °C. (b) Micro-Raman spectra for different concentrations of Sm_2O_3 in Pr_2O_3 (40–60%) at 1000 °C showing the emergence of monoclinic peaks with increasing % of Sm_2O_3. (c) Micro-Raman spectra for different concentrations of Sm_2O_3 in Pr_2O_3 (70–90%) at 1000 °C. The observed patterns show a phase transition from cubic to monoclinic structure and the cubic and monoclinic indices are shown as C(9 2 7), M(4 0 3), etc.

contraction [22]. The Raman shift across the period (lanthanides) reflecting the bonding change as the number of f-electrons increase and the size of the lanthanide atoms decrease. In our case, we have performed the experiment at 1000 °C and here, the wave numbers are around 840 and 430 cm^{-1} respectively for Pr_2O_3 and Sm_2O_3. Fig. 6(c) shows the weaker peaks which loses their intensity and are seen to disappear at higher compositions. With increase in % of Sm, the strongest cubic phase mode shifts to higher wave numbers. The cubic phase is dominant up to 90% and agrees well with the XRD results as reported.

Table 1 lists all the phases of $Pr_2O_3 + Sm_2O_3$ mixed oxide system based on the results of our experiments. The table shows a temperature induced structural transition from cubic to monoclinic phase of mixed oxides. Here, up to 40 wt.% of Sm_2O_3 in Pr_2O_3, the cubic phase was observed. A diphasic region was clearly observed in the compositions ranging between 50 and 70% and after that, it transformed to the monoclinic phase at 80% of Sm_2O_3.

Based on the results of other mixed oxide systems [14,15,23], it has been reported that the contraction of the unit cell and chemical bonding plays an important role in the phase changes of the mixed oxides. Higher temperature studies on the phase transition of these mixed oxides have not been reported.

In summary, we have performed temperature-dependent X-ray diffraction studies on the polymorphic modifications of the mixed rare-earth oxide system Pr_2O_3–Sm_2O_3. This study reveals their C-type cubic crystal structure at lower temperatures (~800 °C) and B-type monoclinic at higher temperatures (~1200 °C). This cubic to monoclinic polymorph helps to identify the phase stability and intermediate phases among those oxides. Along with XRD, micro-Raman experiments were carried out to corroborate our XRD results.

Acknowledgements

D.V. expresses her gratitude to the IGCAR authorities for granting permission to carry out her M.Phil. project work at CMPD, IGCAR. The authors wish to thank Dr. R.K. Dayal, Head, CSTD and Dr. R.V. Subba Rao for extending their Micro-Raman experimental facility. They also wish to thank Shri. V. Kathirvel for his assistance in experimentation and Shri. L.M. Sundaram for his help at various stages of this work. They also extend their thanks to Shri. M. Sekar, Shri N.R. Sanjay Kumar and Shri Y.A. Sorb for valuable discussions. The authors thank Dr. C.S. Sundar, Dr. A.K. Arora and Dr. Baldev Raj for their encouragement and support.

References

[1] C.A.O. Xueqiang, J. Mater. Sci. Technol. 23 (2007) 15.
[2] L. Dayana, N.V. Chandra Shekar, P.Ch. Sahu, B.V. Kumaraswamy, A.K. Bandyopadhyay, M. Rajagopalan, Phil. Mag. Lett. 88 (2008) 473.
[3] A.J. Kenyon, Prog. Quan. Electron. 26 (2002) 260.
[4] M. Zinkevich, Prog. Mater. Sci. 52 (2007) 597.
[5] L. Eyring, in: K.A. Gschneider (Ed.), Handbook on the Physics and Chemistry of Rare Earths, vol. 3, Amsterdam, North Holland, 1979, p. 337.
[6] S. Guhathakurta, H. Singh, Rare Earths, Rare Earth Association of India, 2000, p. 88, chap-5.
[7] P. Maestro, D. Huguenin, J. Alloys Compd. 225 (1995) 520.
[8] T. Justel, J.-C. Krupa, D.U. Wiechert, J. Lumin. 93 (2001) 179.
[9] K.J. Sreeram, S. Kumeresan, S. Radhika, V. John Sundar, C. Muralidharan, B.U. Nair, T. Ramasami, Dyes Pigments 76 (2008) 243.
[10] X.C. Zhang, J.M. Friedrich, M.A. Nearing, L.D. Norton, Soil Sci. Soc. Am. J. 65 (2001) 1508.
[11] H.R. Hoekstra, Inorg. Chem. 5 (1966) 754.
[12] R. McPherson, J. Mater. Sci. 18 (1983) 1341.
[13] S. Sato, R. Takahashi, M. Kobune, H. Gotoh, Appl. Catal. A 356 (2009) 57.
[14] D.J.M. Bevan, E. Summerville, in: K.A. Gschneider (Ed.), Handbook on the Physics and Chemistry of Rare Earths, vol. 3, Amsterdam, North Holland, 1979, p. 401.
[15] G. Brauer, B. Pfeiffer, in: L. Eyring (Ed.), Rare Earth Research III, Gordon and Breach, 1964, p. 573.
[16] P.Ch. Sahu, N.V. Chandra Shekar, N. Subramanian, K. Govinda Rajan, Rev. Sci. Instrum. 66 (1995) 2599.
[17] Y.J. Kim, W.M. Kriven, J. Mater. Res. 13 (1998) 2920.
[18] N. Dilawar, S. Mehrotra, D. Varandani, B.V. Kumaraswamy, S.K. Haldar, A.K. Bandyopadhyay, Mater. Charact. 59 (2008) 462.
[19] J.-F. Martel, S. Jandl, A.M. Lejus, B. Viana, D. Vivien, J. Alloys Compd. 275–277 (1998) 353.
[20] Q. Guo, Y. Zhao, C. Jiang, W.L. Moa, Z. Wang, Solid State Commun. 145 (2008) 250.
[21] J. Gouteron, D. Michel, A.M. Lejus, J. Zarembowitch, J. Solid State Chem. 38 (1981) 288.
[22] M.W. Urban, B.C. Cornilsen, J. Phys. Chem. Solids 48 (1987) 475.
[23] J.-C. Panitz, J.-C. Mayor, B. Grob, W. Durisch, J. Alloys Compd. 303–304 (2000) 340–344.